JOURNAL OF GEOPHYSICAL RESEARCH, VOL. 113, D24211, doi:10.1029/2007JD009538, 2008

Origin of surface and columnar Indian Ocean Experiment (INDOEX) aerosols using source- and region-tagged emissions transport in a general circulation model

S. Verma,[1] C. Venkataraman,[2] and O. Boucher[3,4]

Received 25 October 2007; revised 6 August 2008; accepted 6 October 2008; published 30 December 2008.

[1] We study the relative influence of aerosols emitted from different sectors and geographical regions on aerosol loading in south Asia. Sectors contributing aerosol emissions include biofuel and fossil fuel combustion, open biomass burning, and natural sources. Geographical regions include India (the Indo-Gangetic plain, central India, south India, and northwest India), southeast Asia, east Asia, Africa-west Asia, and the rest of the world. Simulations of the Indian Ocean Experiment (INDOEX), from January to March 1999, are made in the general circulation model of Laboratoire de Météorologie Dynamique (LMD-ZT GCM) with emissions tagged by sector and geographical region. Anthropogenic emissions dominate (54–88%) the predicted aerosol optical depth (AOD) over all the receptor regions. Among the anthropogenic sectors, fossil fuel combustion has the largest overall influence on aerosol loading, primarily sulfate, with emissions from India (50–80%) and rest of the world significantly influencing surface concentrations and AOD. Biofuel combustion has a significant influence on both the surface and columnar black carbon (BC) in particular over the Indian subcontinent and Bay of Bengal with emissions largely from the Indian region (60–80%). Open biomass burning emissions influence organic matter (OM) significantly, and arise largely from Africa-west Asia. The emissions from Africa-west Asia affect the carbonaceous aerosols AOD in all receptor regions, with their largest influence (AOD-BC: 60%; and AOD-OM: 70%) over the Arabian Sea. Among Indian regions, the Indo-Gangetic Plain is the largest contributor to anthropogenic surface mass concentrations and AOD over the Bay of Bengal and India. Dust aerosols are contributed mainly through the long-range transport from Africa-west Asia over the receptor regions. Overall, the model estimates significant intercontinental incursion of aerosol, for example, BC, OM, and dust from Africa-west Asia and sulfate from distant regions (rest of the world) into the INDOEX domain.

Citation: Verma, S., C. Venkataraman, and O. Boucher (2008), Origin of surface and columnar Indian Ocean Experiment (INDOEX) aerosols using source- and region-tagged emissions transport in a general circulation model, *J. Geophys. Res.*, *113*, D24211, doi:10.1029/2007JD009538.

1. Introduction

[2] Aerosol emissions on a regional scale over India arise from fossil fuel combustion (primarily sulfate) and biofuel combustion and open biomass burning (organic carbon, OC, and black carbon, BC) [e.g., *Reddy and Venkataraman*, 2002a, 2002b; *Venkataraman et al.*, 2005, 2006; *Streets et al.*, 2003; *Bond et al.*, 2004]. Sources and geographical regions influencing the atmospheric loading of aerosols during recent observational campaigns have been analyzed qualitatively. Investigators of the Indian Ocean Experiment (INDOEX) used Lagrangian back trajectories to identify different geographical regions influencing their observations [*Mayol-Bracero et al.*, 2002; *Quinn et al.*, 2002; *Dickerson et al.*, 2002] and linked aerosol chemical and optical properties to broad source categories of anthropogenic, dust and sea-salt aerosols. General circulation model (GCM) simulations over south Asia during the INDOEX period with newly available regional emissions information [*Reddy et al.*, 2004; *Verma et al.*, 2007] indicate likely contribution of emissions from regions outside India to aerosol loading over the Indian subcontinent and adjoining oceans. While south Asian emissions were the primary contributor to carbonaceous aerosol surface concentrations over India, these emissions accounted for less than half their

[1]Department of Civil Engineering, Indian Institute of Technology Kharagpur, Kharagpur, India.
[2]Department of Chemical Engineering, Indian Institute of Technology Bombay, Mumbai, India.
[3]Laboratoire d'Optique Atmosphérique, Université des Sciences et Technologies de Lille, CNRS, Villeneuve d'Ascq, France.
[4]Now at Met Office Hadley Centre, Exeter, UK.

0148-0227/08/2007JD009538$09.00

columnar loading, in terms of aerosol optical depth (AOD), over India and adjoining ocean regions [*Reddy et al.*, 2004], implying intrusion of carbonaceous aerosol in elevated plumes. The frequent occurrence of high-altitude aerosol plumes over the INDOEX region is well documented from lidar profiles and aircraft measurement [*Leon et al.*, 2001; *Chazette*, 2003; *Müller et al.*, 2001a, 2001b]. High-resolution GCM simulations to examine the role of sea breeze in aerosol lofting [*Verma et al.*, 2006] showed episodic intrusion of organic carbon aerosols in elevated atmospheric plumes from Africa recirculating over the Indian subcontinent and the northern Indian Ocean.

[3] Elevated aerosol plumes may be transported over large distances so the contribution of emissions from a given geographical region or source may be different for aerosol surface or column concentrations. Again, such regional and source contributions may be varied over different receptor locations in the south Asian region.

[4] The Indian Ocean Experiment linked regional radiative forcing to aerosol loadings and their chemical and optical properties and raised several interesting questions. These include the extent of aerosol incursion into south Asia and the relative influence of local and long-range transported emissions on aerosol loading over the Indian subcontinent and adjoining oceans, during different seasons. In this work, we make quantitative estimates of source and regional contributions to surface and columnar INDOEX aerosols (winter monsoon season), using simulations of the intensive field phase of Indian Ocean Experiment (INDOEX-IFP) in the general circulation model of Laboratoire de Météorologie Dynamique (LMD-ZT GCM), with source- and region-tagged emissions. Source classifications included biofuel combustion for energy, open biomass burning, industrial fossil fuel combustion and natural sources (dust and sea salt). Geographical regions include the Indian subcontinent and adjoining continental regions in Asia and Africa. The specific objectives of the present study are to examine the relative influence of (1) natural and anthropogenic aerosols and (2) emissions from near and distant geographical regions on surface and columnar aerosol loadings over South Asia, during the period of study.

2. Method of Study

2.1. Short Description of the LMD-ZT GCM

[5] The study of region- or source-tagged aerosol transport is carried out with the help of the LMD-ZT general circulation model (GCM), version 3.3. A description of the atmospheric model is given by *Li* [1999] and a specific description of aerosol treatment and atmospheric transport is given by *Boucher et al.* [2002] and *Reddy et al.* [2004]. A short description of the model is presented here. The atmospheric transport in LMDZT GCM is calculated on the basis of the finite-volume second-order scheme for large-scale advection [*van Leer*, 1977; *Hourdin and Armangaud*, 1999] a scheme for turbulent mixing in the boundary layer, and a mass flux scheme for convection [*Tiedtke*, 1989]. The time step is 1 min for resolving the dynamical part of primitive equations. Mass fluxes are cumulated over five time steps so that large-scale advection is applied every 5 min. The physical and chemical parametrization are applied every 30 time steps or 30 min. The different processes are handled through operator splitting. The model has a resolution of 96 points in longitude and 72 points in latitude. There are 19 vertical layers extending from surface up to about 3 hPa, with a hybrid sigma-pressure coordinate, with 5 layers below about 600 hPa and 9 layers above about 250 hPa. A zoom is applied over the Indian region; it is centered at 75°E and 15°N and extends from 50°E to 100°E in longitude and from 5°S to 35°N in latitude. Zoom factors of 4 and 3 are applied in longitude and latitude, respectively, resulting in a resolution of about 1° in longitude and 0.8° in latitude over the zoomed region. Details of aerosol emission inventories incorporated in the model are described in section 2.2.

2.2. Experimental Setup of the LMD-ZT GCM

[6] Geographical regions are identified on the basis of differences in composition of their aerosol emission fluxes and their proximity to the Indian Ocean [*Verma et al.*, 2007]. They include the Indo-Gangetic Plain (IGP), central India (CNI), south India (SI), northwest India (NWI), southeast Asia (SEA), east Asia (EA), Africa-west Asia (AFWA), and rest of the world (ROW). The classified geographical regions are implemented in the GCM. Figure 1 shows the masked regions on GCM zoom grid.

[7] Aerosol sources were classified as fossil fuel (FF), biofuel (BF), open burning (OB), and natural. Sectors for these categories of fuel include coal-fired electric utilities, diesel transport, brick kilns, industrial, transportation, domestic in fossil fuel; wood and crop waste for residential cooking and heating in biofuel; forest biomass and agricultural residues in open burning [*Reddy and Venkataraman*, 2002a, 2002b]. Emissions from natural sources included sulfur from volcanic and biogenic sources [*Boucher et al.*, 2002], terpenes from the vegetation [*Reddy and Boucher*, 2004], dust from arid regions [*Tegen and Fung*, 1995], and sea salt [*Monahan et al.*, 1986]. Aerosol emissions over India (SO_2, BC, and organic matter (OM), and inorganic matter (IOM) (fly-ash emissions from coal combustion)) are from the high-resolution ($0.25° \times 0.25°$) emission inventories of *Reddy and Venkataraman* [2002a, 2002b]. Emissions of SO_2, BC, and organic carbon (OC) from fossil fuel and biomass sources over Asia are from *Streets et al.* [2003]. Global carbonaceous aerosol emissions used here are the same as described by *Reddy and Boucher* [2004].

[8] Carbonaceous aerosols are predominantly emitted in the hydrophobic form, but some fraction of the emissions may be in hydrophilic form as well. Here, we assume that black carbon (BC) emissions from both fossil fuel and biomass burning occur as 80% hydrophobic and 20% hydrophilic, whereas organic matter (OM) emissions occur as 50% hydrophobic and hydrophilic. The aging process of BC and OM is represented by a transfer of the hydrophobic to hydrophilic form with an exponential lifetime of 1.63 days. We provide more details on estimation of the seasonal variability of biomass burning emissions and aerosol parameterization as auxiliary material (see Text S1).[1]

[9] The sulfur cycle has been incorporated and processes of convective transport, wet scavenging, and aqueous-phase chemistry have been parameterized as consistently as pos-

[1] Auxiliary materials are available in the HTML. doi:10.1029/2007JD009538.

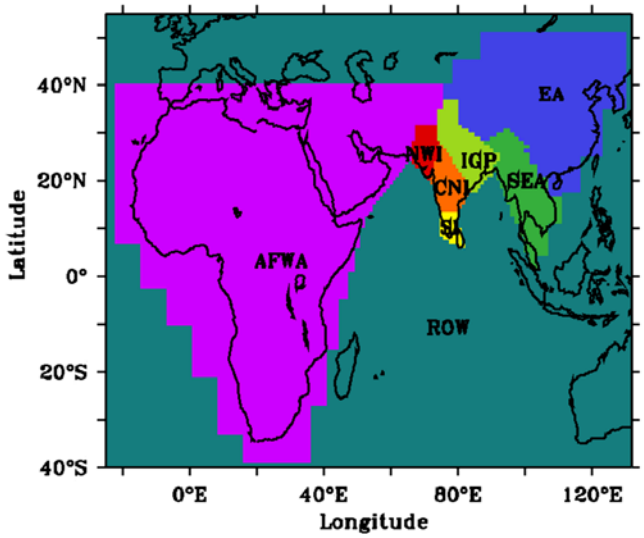

Figure 1. Masked regions on the GCM zoom grid representing tagged geographical regions considered in this study: IGP (light green), CNI (orange), SI (yellow), NWI (red), SEA (green), EA (blue), AFWA (purple), and ROW (dark green).

sible with the model physical parameterization [*Boucher et al.*, 2002]. The concentration of oxidants (except H_2O_2) required in the process of oxidation of SO_2 and the photodissociation rates of H_2O_2 are prescribed from the IMAGES model [*Müller and Brasseur*, 1995]. The H_2O_2 concentration is prognostic as it is significantly affected by sulfur cycle [*Boucher et al.*, 2002; *Boucher and Pham*, 2002]. Aerosol scheme is a mass-only scheme. Aerosol optical properties (mass extinction efficiency, single-scattering albedo, and asymmetry factor) for all aerosol species are computed using Mie theory with prescribed size distributions and refractive indices. We consider the relative humidity (RH) effects on particle size and density of sulfate, hydrophilic OM, and sea salt. The refractive index of sulfate, hydrophilic OM, and sea salt as a function of RH are calculated as the volume weighted average of the refractive indices of each of the aerosol species and water. Aerosol optical properties for all aerosol species are computed assuming an external mixing. More details on the aerosol treatment processes are given as auxiliary material Text S1.

[10] Two sets of experiments were carried out for the present work. In the one setup, aerosol emissions including sulfur dioxide (SO_2), organic matter (OM), black carbon (BC), inorganic matter (IOM), dust, and sea salt (SS) were tagged for each of the classified geographical source regions (IGP, CNI, SI, NWI, SEA, EA, AFWA, ROW). The INDOEX IFP was simulated for each of the geographical region with the emissions outside that region being switched off. In the other setup, aerosol emissions were tagged for each of the combustion (BF, OB, FF) and natural sources and the INDOEX IFP was simulated for each of the combustion and natural source with the other emission sources being switched off. Horizontal model winds are nudged to 6-hourly wind fields from European Centre for Medium-Range Weather Forecasts (ECMWF) with a relaxation time of 0.1 days [*Hauglustaine et al.*, 2004]. This ensures that the simulated transport is reasonably constrained by ECMWF meteorology while the rest of the dynamical and physical processes are driven by model parametrization. GCM simulations with emissions tagged by fuel sources or geographical regions are evaluated to understand the contribution of emissions from the different fuel sources and geographical regions to the aerosol surface mass concentration and optical depth averaged during INDOEX over five receptor regions (Figure 2). The receptor regions as shown in Figure 2 consist of oceanic regions adjoining the Indian subcontinent as Arabian Sea (AS) and Bay of Bengal (BOB), and the remote part of the Indian Ocean consisting of west tropical Indian Ocean (TIOW) and the east tropical Indian Ocean (TIOE). Indian subcontinent (IS) is also taken as one of the receptor regions to analyze the pollution contribution from the Indian and distant geographical regions.

2.3. Model Evaluation

[11] It is to be noted that the INDOEX-IFP was simulated in LMD-GCM and the model has been extensively evaluated [*Reddy et al.*, 2004] with the INDOEX measurements made on various platforms (e.g., ship cruise, satellite). We have used the same version of model with the emissions in the model tagged by geographical regions or fuel sources to evaluate the regional and source contributions to INDOEX aerosols. Comparison of modeled surface mass concentrations for various species of sulfate, black carbon (BC), organic carbon (OC), inorganic matter, and sea salt as a function of latitude for the Ronald Brown cruise showed that the model captured the north to south gradient in measured concentrations with smaller values over the Southern Indian Ocean (SIO) and Intertropical convergence zone (ITCZ) and larger values over the Arabian Sea. However, over the region of largest concentrations (5°N–10°N), modeled estimates averaged between 5°N and 10°N for sulfate and BC concentrations were estimated a factor of 2 to 3 lower than measured values. There is a better

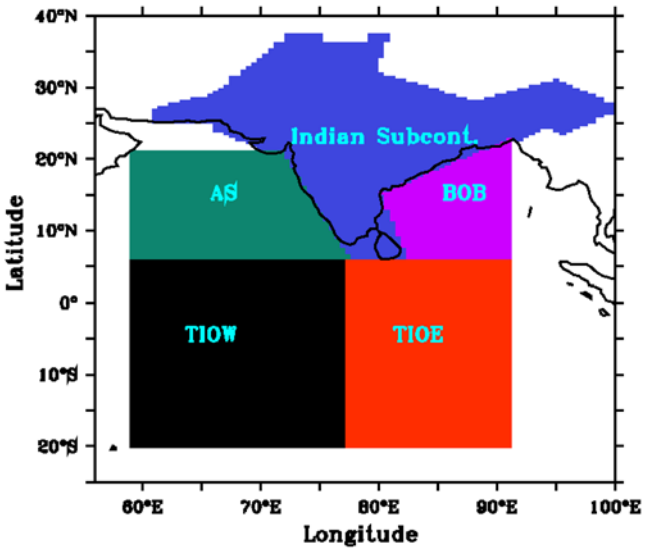

Figure 2. Classified receptor regions: TIOW (black), AS (green), Indian subcontinent (blue), BOB (magenta), and TIOE (red).

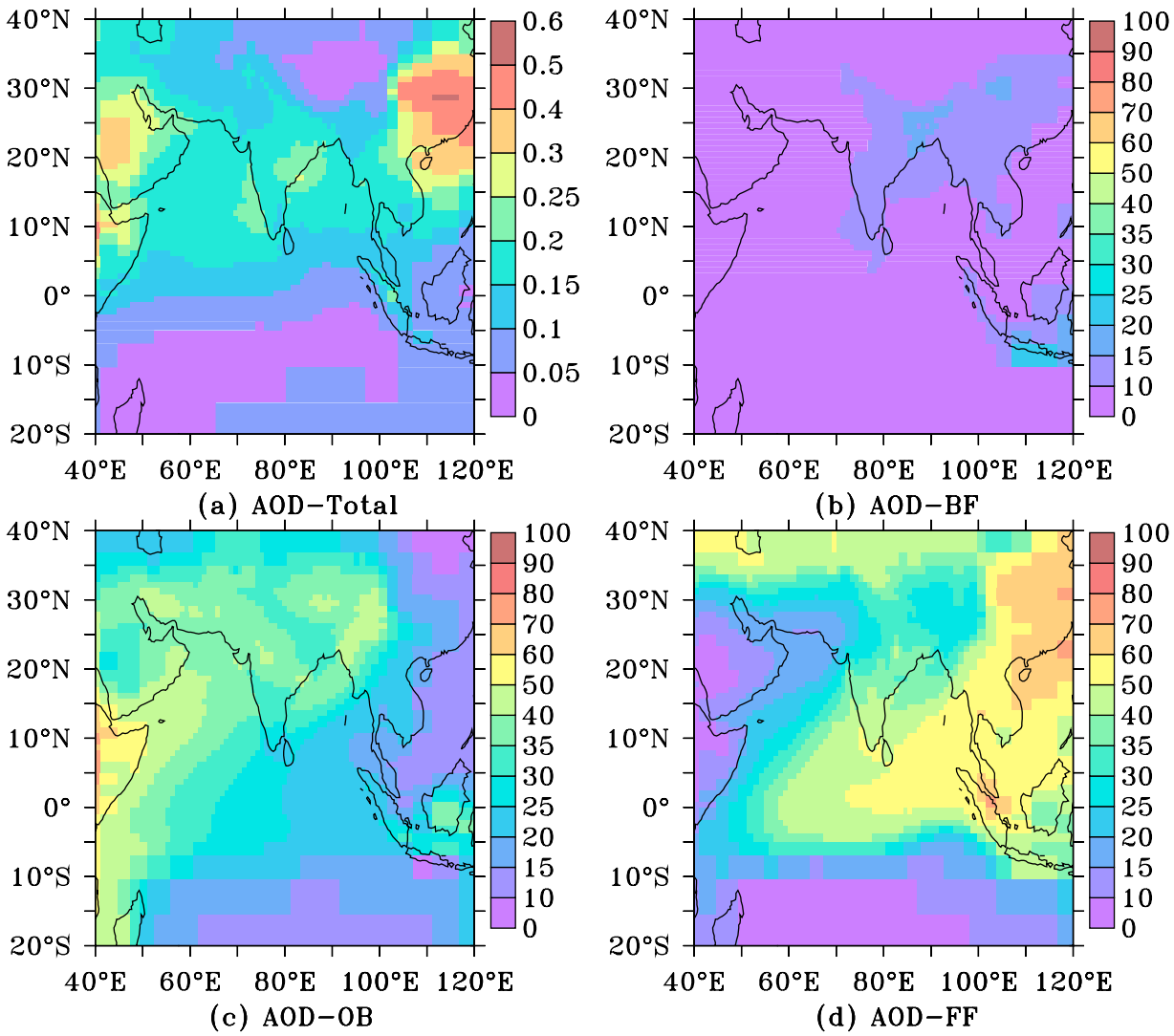

Figure 3. Spatial distribution of (a) total aerosol optical depth at 550 nm and (b) relative contribution (%) of biofuel to total AOD, (c) same as Figure 3b but of open burning, and (d) same as Figure 3b but of fossil fuel combustion during the INDOEX-IFP.

agreement between the modeled OM and sea salt and measurements. Modeled dust was underestimated by a factor of 2 as compared with measurements at Kaashidhoo averaged over the days of March. A comparison of modeled aerosol optical depth (AOD) with measurements onboard the Sagar Kanya during the INDOEX-IFP (see auxiliary material Figure S1) showed that the model agreed relatively well with measurements during the months of January and February except during the days of March (days of the year between 60 to 70) when ship cruised between latitudes 5°N and 15°N where the model values were lower by a factor of 2 to 3. Detailed analysis on model evaluation with INDOEX measurements are presented by *Reddy et al.* [2004]. We also present the spatial distribution of modeled aerosol optical depth (Figure 3a) averaged during the INDOEX-IFP. Following INDOEX-IFP during the year 1999, several field campaigns have been carried out during the recent years over the Indian Ocean and the subcontinent [e.g., *Satheesh et al.*, 2005, 2006; *Vinoj et al.*, 2007] to understand the spatial and temporal features of aerosol characteristics. The model estimates from INDOEX-IFP simulations corresponding to the winter northeast monsoon period from January to March 1999, when compared with the measurements during field campaigns in the subsequent years during the winter (November to April), showed that the model captured well the latitudinal gradient inferred in AOD measurements from northern Arabian Sea to Antarctica during January to April 2006 [*Vinoj et al.*, 2007] and concurs with the low and steady values (less than 0.1) measured in the Southern Indian Ocean (20°S–40°S) and higher AOD values measured north of 20°S (Figure 3a). The modeled AOD (Figure 3a) averaged during January to March 1999 over the Arabian Sea (0.15 to 0.25) and Bay of Bengal (0.15 to 0.2) agrees well with the measurement features compiling data collected from various platforms during the winter from 1995 to 2004, over the Arabian Sea (November to March) (0.29 ± 0.12) [*Satheesh et al.*, 2005], and over Bay of Bengal (October to November) (0.19 ±

0.02) [*Satheesh et al.*, 2006]. The spatial distribution of modeled AOD (Figure 3a) shows AOD over the Indo-Gangetic plain to be in the range 0.15 to 0.25 which is lower by a factor of 2 to 3 in comparison to observational studies from satellite-based measurements [*Jethva et al.*, 2005] which showed AOD averaged during November to January from 2000 to 2003 over the Indo-Gangetic plain to be in the range 0.4 to 0.6. Some discrepancy between modeled and measured values is expected to be due to different yearly time periods used for comparison. We also believe that refinement in the spatial distribution of emissions from residential biomass energy use and the spatial and temporal distribution of emissions from open burning of forest and agricultural biomass may help in closing some of the discrepancy between model predictions and measurements.

[12] We have discussed in detail the reasons of model underestimation in comparison to the measurements during the INDOEX-IFP and possible ways to improve it in our recent work [*Verma et al.*, 2007]. The model underestimation of aerosol surface concentrations and AOD particularly in March was attributed to inaccuracies in ECMWF meteorological analyzes [*Bonazzola et al.*, 2001] which are used to nudge the model, spurious overestimation of precipitation rate in the model over the Arabian Sea and tropical Indian Ocean with a more pronounced effect during the month of March, but there is likely to be as well an underestimation of aerosol sources in the model. We have attached the rainfall pattern from the Global Precipitation Climatology Project (GPCP), as simulated by LMDZT GCM, and from the ECMWF analysis (see auxiliary material Figure S2) and associated discussion (see lines 151 to 163 in auxiliary material Text S1) as auxiliary material with this manuscript. Though model estimates are underestimated, it can be used as a valuable tool to understand the transport of surface and columnar aerosols, and evaluate their origin from the various fuel sources and geographical regions. This is because the pattern of emissions consisting of emission flux composition (SO_2, BC, OM, IOM, dust, sea salt) of regions or combustion sources in the model are expected to be reasonably accurate [*Verma et al.*, 2007]. Emissions have been derived in a consistent way for all the regions although we cannot rule that the emissions are homogeneously underestimated across all regions. Recently, we have also evaluated the source region information from the model with the back trajectory analysis for the days and locations of Sagar Kanya during its INDOEX-IFP cruise. The regional influence evaluated through region-tagged model estimates corroborated the probable source region evaluated through back-trajectory analysis [*Verma et al.*, 2007].

[13] The present work is aimed to assess the origin of surface and columnar INDOEX aerosols from natural or anthropogenic sources, and their transport from adjoining Indian regions or distant geographical regions.

3. Source Contributions to Aerosol Over the Continent and Ocean: Natural Versus Anthropogenic

[14] Table 1 shows the spatially and temporally averaged model estimates of aerosol species surface mass concentration and optical depth from the selected source categories over the receptor regions (TIOW, AS, IS, BOB, TIOE) during the INDOEX-IFP from January to March 1999. Surface concentrations were dominated over the oceanic regions by natural aerosols (69–94%), primarily sea salt, but over the Indian subcontinent by anthropogenic sources (68%). In contrast, AOD over all receptor regions, including the ocean regions, was significantly influenced by anthropogenic aerosols (54–88%). This corroborates the recent observational studies which inferred the presence of high AOD primarily of anthropogenic origin over the Indo-Gangetic plain during the winter (November to January) [*Jethva et al.*, 2005].

[15] Over the Indian subcontinent, anthropogenic sources contribute 68% to surface concentrations and 84% to AOD with an almost equal contribution from fossil fuel sources compared to biofuel and open biomass burning sources put together. We also present the spatial distribution of the total aerosol optical depth (AOD) at 550 nm (Figure 3a) and relative contributions (%) to the total AOD from combustion sources (Figures 3b, 3c, and 3d). A larger influence was seen from open biomass burning on AOD (Table 1 and Figure 3c), and biofuel combustion on surface concentrations (Table 1), consistent with more elevated emissions from open burning, which are introduced into a higher level in the model [*Reddy et al.*, 2004]. Fossil fuel combustion for industrial production and transport had the largest fractional influence, among the anthropogenic sources, on total surface aerosol concentration and AOD (Table 1 and Figure 3d) in all receptor regions. While the influence of this source on surface concentrations is low over ocean regions and modest over the Indian subcontinent, its influence on AOD was substantial over all receptor regions, and higher over the Bay of Bengal (54%) than over the Indian subcontinent (44%). Figure 4 provides a comparison between the relative contribution of a fuel source (shown by different symbols) to surface concentration and columnar loading (taken as AOD) of aerosols averaged over the receptor regions (shown by colors as represented in Figure 2) during the INDOEX-IFP. Data points above the 1:1 line in the scatter plot shown in the Figure 4 indicate a higher relative contribution from the sector (fuel source) in the free and upper atmosphere than at the surface, possibly related to long-range transport.

[16] Fossil fuel combustion had the largest influence on sulfate surface concentrations as well as AOD over all receptor regions (Figure 4a). Fossil fuel sources contribute significantly to IOM (coal fly ash) emissions (Figure 4b), and influence AOD more than surface concentrations in the AS and BOB regions, but influence both in the other receptor regions with a maximum of about 65% over the Indian subcontinent. This is consistent with emissions of SO_2 both from surface sources such as transport, and of SO_2 and IOM from stacks of large industrial point sources like coal-fired electric utilities in the region [*Reddy and Venkataraman*, 2002a]. The greater influence of sulfate over ocean regions than over the subcontinent [*Reddy et al.*, 2004], and its primary origin from fossil fuel combustion, leads to the larger spatial influence of this source on AOD, including ocean regions. The extent of incursion of fossil fuel emissions from outside India is discussed in section 4.

[17] Biofuel combustion as a domestic source of energy has a significant influence on the Indian subcontinent

Table 1. Source Contributions to Aerosol Surface Mass Concentration and AOD at 550 nm (×100) Averaged During the INDOEX Over the Receptor Regions[a]

	Fuel Source							
	Anthropogenic		Biofuel		Open Burning		Fossil Fuel	
Receptor Region	Sur	AOD	Sur	AOD	Sur	AOD	Sur	AOD
TIOW	1.7(11)	3.4(60)	0.2(1)	0.4(7)	0.6(4)	1(18)	0.9(6)	2(35)
AS	3.7(23.6)	11(84)	0.5(0.6)	1(10)	1.2(8)	4(34)	2(15)	6(40)
India	7.6(68)	10(88)	2(18)	2(14)	1.6(14)	3(30)	4(36)	5(44)
BOB	5.2(31)	13(88)	0.7(4)	2(12)	1.5(9)	3(22)	3(18)	8(54)
TIOE	1.3(5.5)	4.4(54)	0.1(0.5)	0.4(7)	0.5(2)	1(15)	0.7(3)	3(32)

[a]Aerosol surface mass concentration (Sur) given in $\mu g\ m^{-3}$. The values within the brackets represent the percentage contributions.

affecting surface aerosol concentrations to 18% and AOD to 14%, with a smaller contribution of 10–12% on AOD in the AS and BOB regions (Table 1 and Figure 3b). This is consistent with biofuel combustion being a dispersed source leading to surface emissions and less prone to long-range transport, unless lofted above the boundary layer by air mass convergence and lofting, for example, shown along the west coast of India during parts of the INDOEX-IFP [*Verma et al.*, 2006]. Biofuel combustion contributes 35–55% of BC surface concentrations and AOD in all receptor regions (Figure 4c) with the largest influence over the Indian subcontinent. While the large influence of biofuel combustion on surface BC concentrations is consistent with its predominance as a source of BC emissions from India [*Venkataraman et al.*, 2005], it is interesting that it also influences columnar BC over the subcontinent to a large extent. Biofuel combustion influences OM surface concentrations (Figure 4d), but contributes less to OM AOD (scatters lie below the 1:1 line) implying a higher relative contribution from BF at the surface as compared to the free and upper atmosphere. It contributes negligibly to sulfate and IOM, making it primarily an important source of both surface and columnar BC and surface OM in the region.

[18] Open burning of forest and crop residues influences total aerosol surface concentration (14%) over the Indian subcontinent and AOD (15–34%) over all receptor regions (Table 1 and Figure 3c). It also has a larger influence on AOD than aerosol surface concentrations (Table 1 and Figures 4c and 4d; BC and OM scatters from OB source lie above 1:1 line, indicating a higher relative contribution from OB in free and upper atmosphere as compared to the surface), consistent with thermal lofting of emissions from open fires. It has a larger influence on OM than BC, based on the composition of aerosols from large fires, which contain more OC than BC, reflected in its larger contribution in the Indian emission inventory to OC than BC [*Venkataraman et al.*, 2006]. Its influence on total and carbonaceous aerosol AOD is especially large over the AS region (Figures 4c and 4d) consistent with measurements of pollutants originating from biomass burning in elevated layer plumes measured from aboard the C-130 aircraft [*Mayol-Bracero et al.*, 2002; *Gabriel et al.*, 2002]. The regional origin of this source is largely outside the Indian subcontinent as discussed in section 4.

[19] In summary, significant influences of emissions source categories on aerosols include fossil fuel emissions on sulfate and IOM concentrations and AOD, biofuel and open biomass burning on BC and OM surface concentrations and open biomass burning on BC and OM optical depth. This is consistent with the recent studies by *Koch et al.* [2007] using the Goddard Institute for Space Studies (GISS) GCM which showed large contribution of sulfate

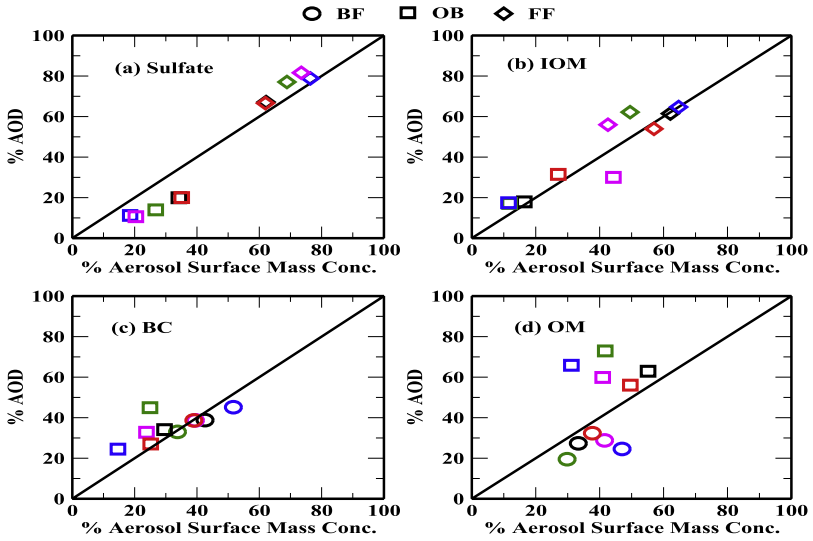

Figure 4. Scatterplot of the percentage contribution of emissions from biofuel combustion for energy, open biomass burning, and fossil fuel combustion to the time mean and spatial mean of aerosol surface mass concentration and optical depth during INDOEX for (a) sulfate, (b) IOM, (c) BC, and (d) OM. Two sources are shown in each plot, and the third can be computed. The colors represent the receptor regions: TIOW, black; AS, green; India, blue; BOB, magenta; and TIOE, red.

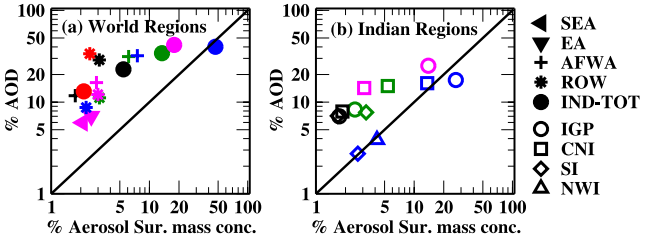

Figure 5. Scatterplot of the percentage contribution of (a) world regions (IND-TOT, SEA, EA, AFWA, and ROW), and (b) Indian regions to the anthropogenic (sum of BC, OM, IOM, and sulfate) aerosol surface mass concentration and optical depth at 550 nm averaged during January to March 1999 over the receptor regions. The colors represent the receptor regions: TIOW, black; AS, green; India, blue; BOB, magenta; and TIOE, red. IND-TOT represents the contribution from all Indian regions (sum of IGP, CNI, SI, and NWI).

from industrial and power sector, BC from residential sector, and OM from biomass burning.

4. Regional Contributions to Aerosol: Adjoining Regions Versus Distant Regions

[20] We further evaluate the contribution of emissions from the different geographical regions, defined in section 2, to the aerosol surface and column loading, as discussed in section 3. The contribution of emissions arising from India (IND-TOT), and other regions (east Asia EA, southeast Asia SEA, Africa and west Asia AFWA, and the rest of the world ROW) are shown for the total anthropogenic (sum of BC, OM, sulfate, IOM) aerosol (Figure 5a) along with a further breakdown (Figure 5b) of Indian emissions to the Indo-Gangetic Plain (IGP), central India (CI), south India (SI) and northwest India (NWI). The sum of emissions from all Indian regions (IND-TOT) has the largest influence over receptor regions of India (blue), Arabian Sea (green) and Bay of Bengal (magenta) with a larger influence on AOD than surface concentrations over the ocean regions, but an equal influence over the continent, which had higher mean surface concentrations of aerosols (Table 1). In addition, anthropogenic AOD is almost equally contributed by the emissions from Africa and west Asia (about 30%) over the Arabian Sea and the Indian subcontinent. Interestingly, emissions from distant regions, for example, "rest of the world," contribute primarily to anthropogenic AOD over the west (TIOW) and the east tropical Indian ocean (TIOE) with a secondary contribution from India. Among the Indian regions (Figure 5b), the emissions from the Indo-Gangetic Plain primarily contribute to the anthropogenic surface and columnar aerosol loading over the Bay of Bengal. However, the Arabian Sea and west tropical Indian Ocean are impacted by almost equal contributions from the Indo-Gangetic Plain, Central India, and South India. The emissions from both the central India and Indo-Gangetic Plain contribute almost equally to the anthropogenic aerosol loading over the Indian subcontinent.

[21] Figure 6 represents the contributions from emissions arising from India (IND-TOT), and other regions (east Asia EA, southeast Asia SEA, Africa and west Asia AFWA, and the rest of the world ROW) for the four anthropogenic aerosol species (Figure 6, left) along with a further breakdown (Figure 6, right) of Indian emissions to the Indo-Gangetic Plain (IGP), central India (CI), south India (SI) and northwest India (NWI). The scatter plot as shown in the Figure 6 provides a comparison between the relative contribution of emissions from a region (shown by different symbols) to surface concentration and columnar loading (taken as AOD) of aerosols averaged over the receptor regions (shown by colors as represented in Figure 2) during the INDOEX-IFP. As mentioned earlier, data points above the 1:1 line in the scatter plot indicate a higher relative contribution from the region in the free and upper atmosphere than at the surface, possibly related to long-range transport. Figures 7 and 8 show the spatial distribution of aerosol optical depth at 550 nm (Figures 7a, 7b, 8a, and 8b) and the relative contributions (%) from key geographical regions (regions which show significant contribution) for sulfate, BC, OM, and dust, respectively.

[22] Indian emissions (IND-TOT) significantly influence sulfate loadings (Figures 6a and 7c) over the receptor regions in the Indian subcontinent, the Arabian Sea and the Bay of Bengal (see caption of Figure 6 for color code) with a secondary contribution from the rest of the world (ROW). In contrast, sulfate loadings in the western and eastern tropical Indian Ocean are primarily influenced by emissions from the rest of the world (ROW) with a secondary contribution from Indian emissions (Figures 6a and 7g). This influence is somewhat more on sulfate AOD than surface concentrations, consistent with its long-range transport in elevated atmospheric layers. Interestingly, emissions from southeast Asia and east Asia (Figure 7e) influenced sulfate concentrations mainly over the Bay of Bengal and did not contribute significantly to sulfate concentrations over the Indian subcontinent and other ocean regions during the winter monsoon of 1999, implying sulfate transport from more distant geographical regions. Among Indian regions, the Indo-Gangetic Plain and central India (Figure 6b) are primary regions of origin for sulfate aerosols where fossil fuel combustion exists in coal-fired electric utilities, refineries, cement and metals production in India [*Reddy and Venkataraman*, 2002a]. While the IGP influence on surface sulfate (40%) is somewhat larger than that on sulfate AOD, emissions from CNI affect almost equally to both surface and columnar sulfate (20%). This probably reflects the higher SO_2 flux from surface sources in the IGP than in CNI [*Reddy and Venkataraman*, 2002a]. Emissions of SO_2 from the large industrial sources in both regions are emitted into a higher level in the model [*Reddy et al.*, 2004] and would have a greater influence on AOD and long-range transport.

[23] The emissions of inorganic matter in the GCM are only from the Indian emissions [*Reddy and Venkataraman*, 2002a, 2002b] with no emissions assigned to the other world regions, because of unavailability of a global emission inventory. Hence, as represented in Figure 6c, only Indian emissions contribute to IOM loading in all receptor regions. Among the Indian regions (Figure 6d), the Indo-Gangetic plain mainly contribute to the IOM surface and columnar loadings over the Bay of Bengal, east tropical Indian Ocean, and the Indian subcontinent. However, the

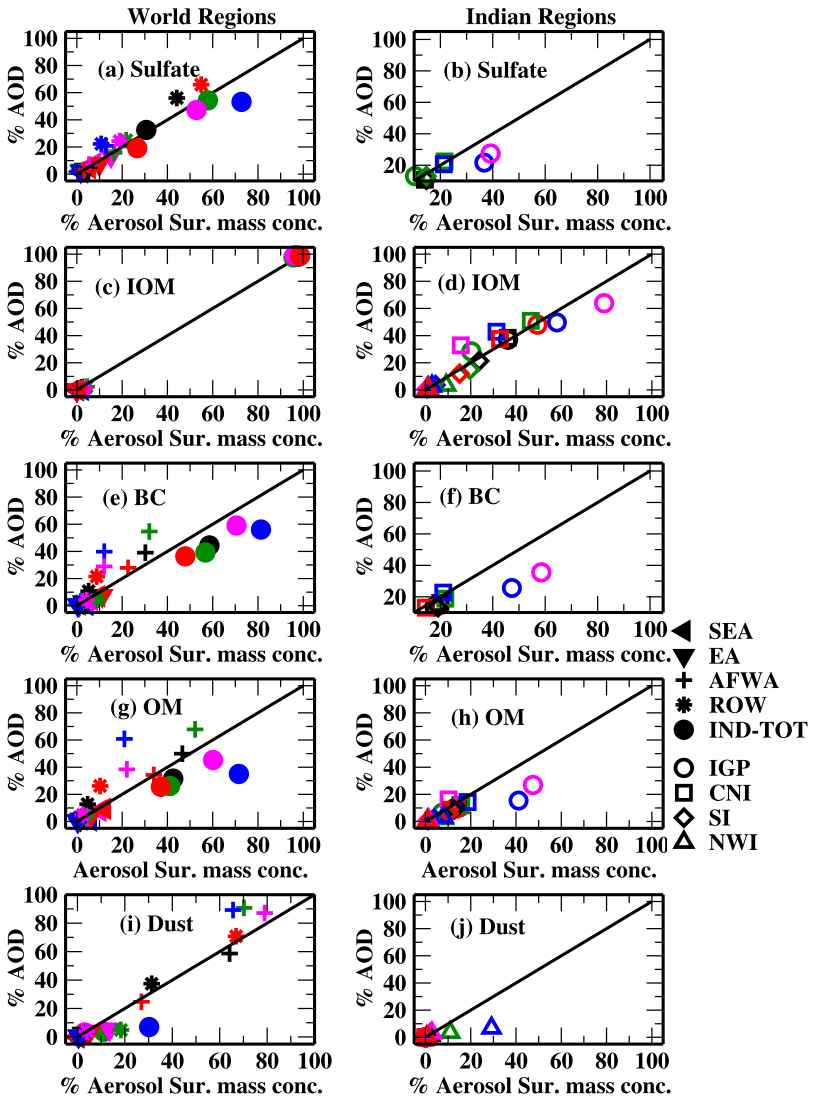

Figure 6. (left) Scatterplot of the percentage contributions of world regions (IND-TOT, SEA, EA, AFWA, and ROW) to aerosol surface mass concentration and optical depth averaged during January to March 1999 over the receptor regions due to (a) sulfate, (c) IOM, (e) OM, (g) BC, and (i) dust. (b, d, f, h, and j) Same as left plots but from Indian regions (IGP, CNI, SI, and NWI). The receptor regions are represented by different symbols and colors (same as in Figure 2) as following: TIOW (circle and black), AS (diamond and green), India (square and blue), BOB (triangle up and magenta), and TIOE (triangle down and red). The fill inside the symbols (see legends) represents the different source regions. IND-TOT represents the contribution from all Indian regions (sum of IGP, CNI, SI, and NWI).

central India contributes primarily to the IOM surface and columnar loadings over the Arabian Sea. The west tropical Indian Ocean is equally influenced by contributions from both the Indo-Gangetic Plain and the central India. Similar to the sulfate transport, the emissions from central India have a higher impact to the aerosol optical depth as compared to the surface mass concentration.

[24] Emissions from Africa and west Asia significantly influence carbonaceous aerosols (Figures 6e and 6g), especially organic matter loadings, over all receptor regions during the winter monsoon of 1999. The spatial distribution of relative contributions (%) to the AOD due to BC and OM originating from Africa and west Asia are represented in Figures 7h and 8e respectively. Biomass burning in woodland, shrub land and broad leaf forest are likely from northern sub-Saharan Africa during December to March [*Tansey et al.*, 2004; *Simon et al.*, 2004]. Transport channels from Africa into the Indian region during the INDOEX period have been suggested in earlier studies [*Rasch et al.*, 2001; *Reddy et al.*, 2004; *Verma et al.*, 2006]. The simulations with region-tagged emissions here present the first quantitative estimate of the extent of carbonaceous aerosol incursion from Africa and west Asia into the Indian region during this period. Emissions from Africa and west Asia are important contributors to surface BC (Figure 6e) over the Arabian Sea and the western tropical Indian Ocean (30–

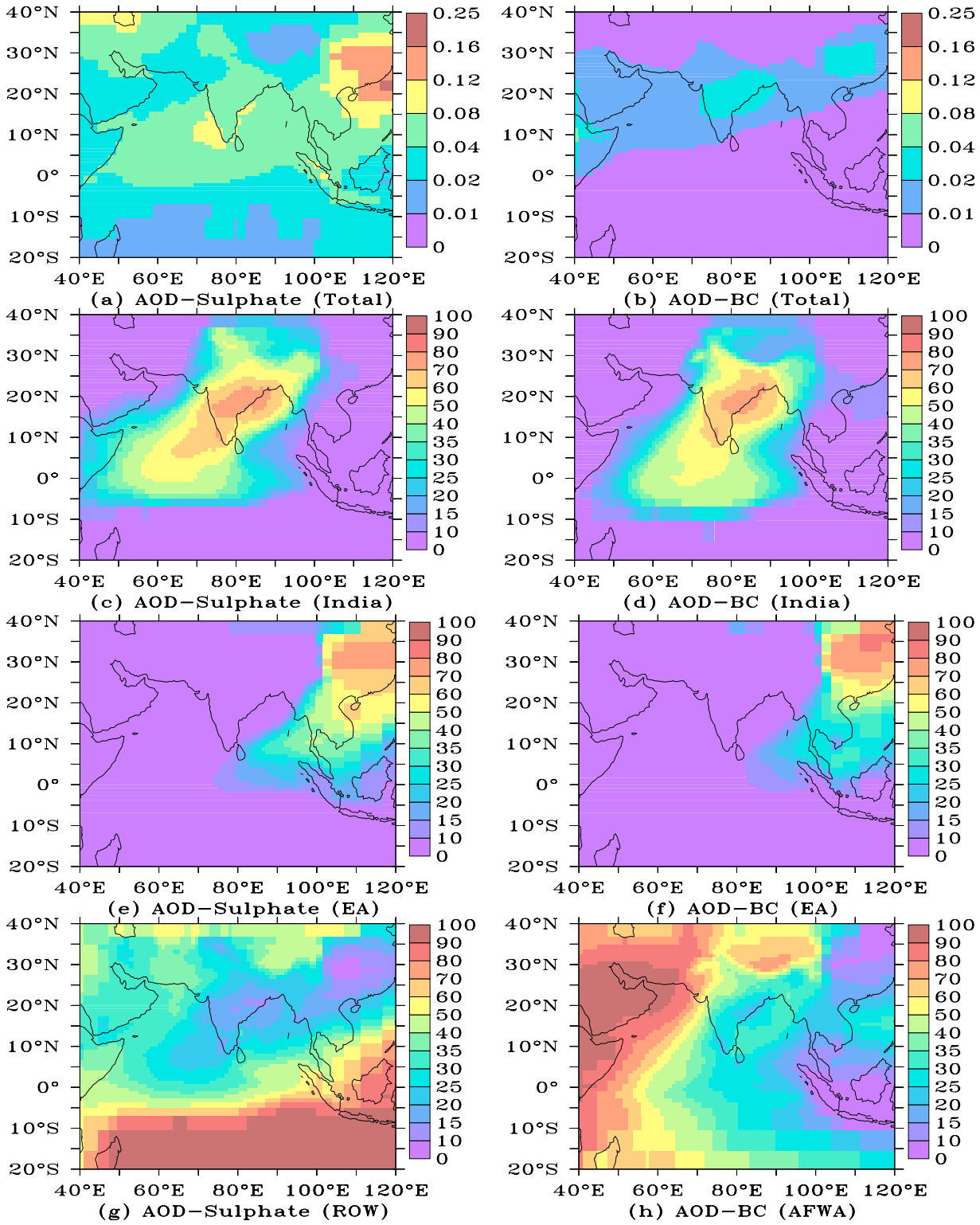

Figure 7. Spatial distribution of (a) total aerosol optical depth due to sulfate at 550 nm, (b) total aerosol optical depth due to BC at 550 nm, (c) relative contribution (%) to the AOD due to sulfate for the aerosols originating from India (sum of IGP, CNI, SI, and NWI), (e) same as Figure 7c but from east Asia, (g) same as Figure 7c but from ROW, (d) relative contribution to the AOD due to BC for the aerosols originating from India, (f) same as Figure 7d but from east Asia, and (h) same as Figure 7d but from Africa-west Asia.

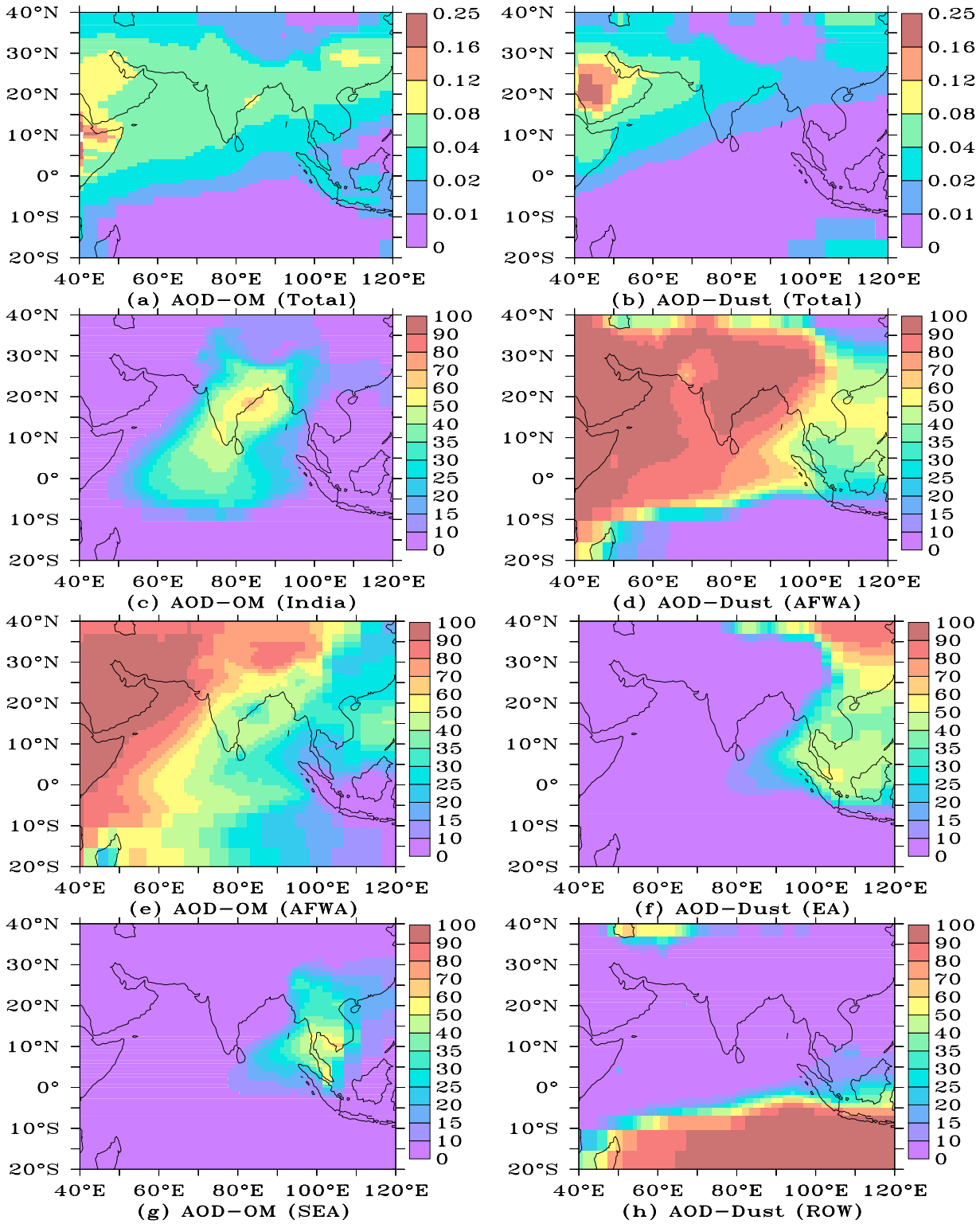

Figure 8. Spatial distribution of (a) total aerosol optical depth due to OM at 550 nm, (b) total aerosol optical depth due to dust at 550 nm, (c) relative contribution (%) to the AOD due to dust for the aerosols originating from India (sum of IGP, CNI, SI, and NWI), (e) same as Figure 8c but from Africa-west Asia, (g) same as Figure 8c but from southeast Asia, (d) relative contribution to the AOD due to dust for the aerosols originating from Africa-west Asia, (f) same as Figure 8d but from east Asia, and (h) same as Figure 8d but from ROW.

Table 2. Relative Contributions of the Classified Geographical Source Regions to the AOD at 550 nm Averaged Over the Same Regions as the Receptor Regions[a]

Source Region	Receptor Region				
	India	SEA	EA	AFWA	ROW
India	40	14	7	1	2
SEA	1	20	5	0	1
EA	1	23	51	0	4
AFWA	46	20	15	88	12
ROW	12	23	22	11	81

[a]Relative contributions are given as percent. Geographical source regions are shown in Figure 1.

40%) and BC optical depth (Figures 6e and 7h) over all receptor regions (≈30–60%). Emissions from Africa-west Asia strongly influence OM optical depth (Figures 6g and 8e) over the Indian subcontinent, Arabian Sea and the western tropical Indian Ocean (50–60%) and OM surface concentrations (≈50%) in the ocean regions (Figure 6g). It is to be noted that most of the points for BC and OM originating from Africa and west Asia (plus symbol in Figures 6e and 6g) lie above the 1:1 line indicating a higher relative contribution from Africa-west Asia in the free and upper atmosphere than at the surface in corroboration to the recent studies by *Koch et al.* [2007] inferring the transport of lofted layer of aerosols from Africa over the southern hemisphere. This indicates significant incursion of long-range transported carbonaceous aerosols in elevated atmospheric layers over the Indian subcontinent. The emissions from southeast Asia (Figure 8g) influence OM concentrations (as high as 30%) mainly over the parts of Bay of Bengal and east tropical Indian ocean.

[25] Figures 7d and 8c show the spatial distribution of the relative contribution (%) to AOD due to BC and OM, respectively, originating from India (sum of IGP, CNI, SI, NWI). Emissions from India are the largest contributor to surface BC (Figure 6e) over the subcontinent and the Bay of Bengal (70–80%). Emissions from India strongly influence OM surface concentrations (50–60%) (Figure 6g), especially over the subcontinent and Bay of Bengal, but have less impact on AOD due to OM (Figures 6g and 8c). Interestingly, most points related to aerosols originating from IND-TOT lie below the 1:1 line (Figure 6g) indicating a higher relative contribution from India at the surface than in the free and upper atmosphere. This is consistent with large organic matter fluxes from surface sources such as biofuel combustion and brick making in the Indo-Gangetic Plain [*Reddy and Venkataraman*, 2002a, 2002b; *Venkataraman et al.*, 2005] and the transport patterns into the Bay of Bengal. Among Indian regions, the Indo-Gangetic Plain is the largest contributor to surface BC (60%), especially in the Bay of Bengal (Figure 6f), consistent with transport patterns pointed out in several studies [e.g., *Verver et al.*, 2001] from the IGP into the Bay of Bengal and over south India. The IGP (Figure 6h) influences OM surface concentrations (40 to 50%) and the CNI has a larger influence on OM AOD. Biofuel combustion for energy is predominant in the IGP, while forest burning takes place in central India in March [*Venkataraman et al.*, 2005, 2006].

[26] We also evaluate the relative contributions (see Table 2) of emissions from the classified geographical source regions (shown in Figure 1) to the AOD spatially averaged over themselves. Table 2 shows that emissions from each region have the largest influence on AOD over the same region. Indian emissions have significant effects on AOD over India (40%), a small effect over southeast Asia (14%) and east Asia (7%), and negligible effects over Africa-west Asia (1%) and rest of the world (2%). The spatial distribution of relative (%) contributions to AOD from India as represented in Figures 7c, 7d, and 8c show that the plume from the Indian regions has maximum impact within the zone of 10°S to 40°N and from 40°E to 100°E (which includes our defined receptor regions over oceanic regions of the ROW including TIOW, AS, BOB and TIOE; details of Indian contributions which ranges from about 30% to 60% are discussed in the previous paragraphs). This shows that emissions from India have a large regional impact but a minimal impact on other parts of the world continental and oceanic regions (excluding Indian subcontinent and Ocean), consistent with a recent study by *Koch et al.* [2007].

[27] We also show the contributions from different regions to the natural aerosols mainly composed of dust (Figures 6i and 6j) and sea salt over the receptor regions. The spatial distribution for AOD due to dust at 550 nm and relative contributions (%) from key geographical regions are shown in Figure 8 (right). Figure 8b shows that the dust AOD has a larger influence over the Arabian Sea and the Indian subcontinent as compared to the other receptor regions in corroboration with the recent observational studies inferring the presence of high dust aerosols over India during March through retrieving regional characteristics of dust aerosols from the infrared radiance acquired from METEOSAT-5 [*Deepshikha et al.*, 2006a, 2006b]. Sea salt, primarily from oceanic regions (contained in the rest of the world category (figure not shown)), dominate the surface mass concentration over oceanic receptor regions as expected. It is also interesting to note the sea-salt transport from oceanic regions of rest of the world over the Indian subcontinent with a much higher impact over the sea-salt AOD as compared to the surface concentration indicating its transport in higher layer over the subcontinent. Dust is primarily transported from Africa and west Asia over the Arabian Sea, Bay of Bengal and the Indian subcontinent (Figures 6i and 8d) with a small contribution (30%) from east Asia (Figure 8f) over the parts of Bay of Bengal and east tropical Indian Ocean. Dust loadings from Africa and west Asia also shows a higher influence to the optical depth as compared to the surface mass concentration (Figure 6i) indicating its transport in higher layers. Interestingly, dust over the east tropical Indian ocean is primarily contributed from rest of the world (Figures 6i and 8h) with a somewhat higher influence to columnar as compared to the surface dust loadings. Among the Indian regions (Figure 6j), northwest India contributes to about 30% to surface dust concentration over the Indian subcontinent.

[28] In summary, emissions from different regions influence surface and columnar loadings of different aerosol species. India and distant regions, (i.e., "rest of the world") influence sulfate concentrations and AOD. India influences surface concentrations of BC and OM, while Africa-west

Asia influences BC and OM AOD. Africa-west Asia contributes to dust concentrations and AOD. The model estimates the presence of significant intercontinental transport of aerosol, for example, BC, OM and dust from Africa-west Asia in higher layers over the Indian subcontinent and sulfate from rest of the world over the Indian Ocean. This could be a reason why measurements, especially high concentrations of carbonaceous aerosols, could not be fully explained by current Indian emissions inventory estimates [*Reddy and Venkataraman*, 2002a, 2002b].

5. Conclusions

[29] The extent of aerosol incursion into south Asia and the relative influence of local and long-range transported emissions was investigated during the winter monsoon of 1999 (January to March 1999) corresponding to the INDOEX-IFP, using region- and source-tagged emissions transport in the LMD-ZT GCM, aggregated over five receptor regions of the tropical Indian Ocean-west (TIOW), Arabian Sea (AS), Indian subcontinent (India), Bay of Bengal (BOB), and tropical Indian Ocean-east (TIOE). The model estimates showed the presence of distinct source and regional contribution to the surface and columnar carbonaceous aerosols over the receptor regions which could be the reason for the lack of reconciliation between INDOEX measurements and local emission inventory estimates [*Reddy and Venkataraman*, 2002a, 2002b]. Biofuel combustion for energy is the primary source of surface black carbon and organic matter and of black carbon AOD over the Indian subcontinent. Open burning of forest and crop residues is the prime contributor to organic matter aerosols and influences AOD more than surface concentrations over all the receptor regions, with the largest impact over the Arabian Sea.

[30] Model estimates tagged with the geographic regions showed that the surface BC (60–80%) is mainly contributed by emissions from the Indian regions. In contrast, emissions from Africa and west Asia significantly influenced the carbonaceous aerosol optical depth with their transport in elevated atmospheric layers. They were important contributors to surface BC (30–40%) and OM (50%) over the Arabian Sea and west tropical Indian Ocean and were the prime contributors to OM optical depth (60–70%) over all the receptor regions including the Indian subcontinent. Industrial fossil-fuel combustion transported from the Indian regions (40–60%) dominate sulfate aerosols over all the receptor regions. However, emissions from rest of the world largely influenced the sulfate (50–60%) optical depth over the west and east tropical Indian Oceanic regions.

[31] Among the Indian regions, the Indo-Gangetic Plain, is the largest contributor to anthropogenic surface mass concentration and AOD, especially over the Bay of Bengal and the subcontinent. Aerosol loadings over the Arabian Sea and tropical Indian Oceanic regions are influenced almost equally from Indo-Gangetic Plain, central India, and south India. Emissions from central India also showed a larger influence to columnar aerosol as compared to the surface, especially over the Bay of Bengal. Dust aerosols were mainly contributed through the long-range transport from Africa and west Asia over all the receptor regions except over the east tropical Indian Ocean where it was primarily contributed from rest of the world. Model estimates showed that the emissions from India had a large regional impact but a minimal impact on the other parts of the world continental and oceanic regions (excluding Indian subcontinent and Ocean).

[32] In summary, three main source-receptor links were identified for aerosol species over the Indian Ocean and Indian subcontinent: (1) open biomass burning from Africa-west Asia and biofuel and fossil fuel sources from India contributing black carbon and organic matter (2) India emissions transported over synoptic scales influencing sulfate over India and adjoining oceans, but emissions from distant regions transported over intercontinental scales to the tropical Indian Ocean, and (3) dust from Africa-west Asia over most of the receptor domain, and distant dust sources over the east tropical Indian Ocean.

[33] The present work addressed the origin of aerosols in terms of their emission sources and geographic region during the INDOEX-IFP (Indian winter monsoon season) which remained to be understood over the Indian Ocean and subcontinent. However, sensitivity studies of the aerosol transport simulations with GCM using a refined temporal and spatial distribution of emissions and meteorological fields need to be further undertaken to assess confidence intervals for the source and regional attribution to the aerosols examined in the present study.

[34] **Acknowledgments.** Computing resources at Indian Institutes of Technology Kharagpur and Bombay were supported through a grant from the Sponsored Research and Industrial Consultancy (SRIC) and Indian Ministry for Human Resource Development respectively. A significant part of this work was accomplished through computing time provided by the "Institut du Développement et des Ressources en Informatique Scientifique" (IDRIS) of the CNRS under projects 031167 and 041167. S. Verma acknowledges support from START and the French Embassy in India for her two visits to LOA (France). This study is part of a collaborative project also supported by the Indo-French Centre for the Promotion of Advanced Research (IFCPAR).

References

Bonazzola, M., L. Picon, H. Laurent, F. Hourdin, G. Sèze, H. Pawlowska, and R. Sadourny (2001), Retrieval of large-scale wind divergences from infrared Meteosat-5 brightness temperatures over the Indian Ocean, *J. Geophys. Res.*, *106*(D22), 28,113–28,128.

Bond, T. C., D. G. Streets, S. D. Fernandes, S. M. Nelson, K. F. Yarber, J.-H. Woo, and Z. Klimoni (2004), A technology-based global inventory of black and organic carbon emissions from combustion, *J. Geophys. Res.*, *109*, D14203, doi:10.1029/2003JD003697.

Boucher, O., and M. Pham (2002), History of sulphate aerosol radiative forcings, *Geophys. Res. Lett.*, *29*(9), 1308, doi:10.1029/2001GL014048.

Boucher, O., M. Pham, and C. Venkataraman (2002), Simulation of the atmospheric sulphur cycle in the Laboratoire de Météorologie Dynamique general circulation model: Model description, model evaluation and global and European budgets, *Note Sci. 23*, 27 pp., Inst. Pierre Simon Laplace, Paris. (Available at http://www.ipsl.jussieu.fr/poles/Modelisation/NotesSciences.htm.)

Chazette, P. (2003), The monsoon aerosol extinction properties at Goa during INDOEX as measured with lidar, *J. Geophys. Res.*, *108*(D10), 4187, doi:10.1029/2002JD002074.

Deepshikha, S., S. K. Satheesh, and J. Srinivasan (2006a), Dust aerosols over India and adjacent continents retrieved using METEOSAT infrared radiance Part I: Sources and regional distribution, *Ann. Geophys.*, *24*, 37–61.

Deepshikha, S., S. K. Satheesh, and J. Srinivasan (2006b), Dust aerosols over India and adjacent continents retrieved using METEOSAT infrared radiance Part II: Quantification of wind dependence and estimation of radiative forcing, *Ann. Geophys.*, *24*, 63–79.

Dickerson, R. R., M. O. Andreae, T. Campos, O. L. Mayol-Bracero, and C. Neusuess (2002), Analysis of black carbon and carbon monoxide observed over the Indian Ocean: Implications for emissions and photo-

chemistry, *J. Geophys. Res.*, *107*(D19), 8017, doi:10.1029/2001JD000501.
Gabriel, R., O. Mayol-Bracero, and M. Andreae (2002), Chemical characterization of submicron aerosol particles collected over the Indian Ocean, *J. Geophys. Res.*, *107*(D19), 8005, doi:10.1029/2000JD000034.
Hauglustaine, D. A., F. Hourdin, L. Jourdain, M.-A. Filiberti, S. Walters, J.-F. Lamarque, and E. A. Holland (2004), Interactive chemistry in the Laboratoire de Météorologie Dynamique general circulation model: Description and background troposphere chemistry evaluation, *J. Geophys. Res.*, *109*, D04314, doi:10.1029/2003JD003957.
Hourdin, F., and A. Armangaud (1999), The use of finite-volume methods for atmospheric advection of trace species. Part 1: Test of various formulations in a general circulation model, *Mon. Weather Rev.*, *127*, 822–837.
Jethva, H., S. K. Satheesh, and J. Srinivasan (2005), Seasonal variability of aerosols over the Indo-Gangetic basin, *J. Geophys. Res.*, *110*, D21204, doi:10.1029/2005JD005938.
Koch, D., T. C. Bond, D. Streets, N. Unger, and G. R. van der Werf (2007), Global impacts of aerosols from particular source regions and sectors, *J. Geophys. Res.*, *112*, D02205, doi:10.1029/2005JD007024.
Leon, J.-F., et al. (2001), Large-scale advection of continental aerosols during INDOEX, *J. Geophys. Res.*, *106*(D22), 28,427–28,440.
Li, Z.-X. (1999), Ensemble atmospheric GCM simulation of climate interannual variability from 1979 to 1994, *J. Clim.*, *12*, 986–1001.
Mayol-Bracero, O., R. Gabriel, M. Andreae, T. Kirchstetter, T. Novakov, J. Ogren, P. Sheridan, and D. Streets (2002), Carbonaceous aerosols over the Indian Ocean during INDOEX: Chemical characterisation, optical properties and probable sources, *J. Geophys. Res.*, *107*(D19), 8030, doi:10.1029/2000JD000039.
Monahan, E. C., D. E. Spiel, and K. L. Davidson (1986), A model of marine aerosol generation via whitecaps and wave disruption, in *Oceanic Whitecaps and Their Role in Air-Sea Exchange Processes*, edited by E. C. Monahan and G. M. Niocaill, pp. 167–174, D. Riedel, Norwell, Mass.
Müller, J.-F., and G. P. Brasseur (1995), IMAGES: A three-dimensional chemical transport model of the global troposphere, *J. Geophys. Res.*, *100*(D8), 16,455–16,490.
Müller, D., K. Franke, F. Wagner, D. Althausen, A. Ansmann, and J. Heintzenberg (2001a), Vertical profiling of optical and physical particle properties over the tropical Indian Ocean with six-wavelength lidar: 1. Seasonal cycle, *J. Geophys. Res.*, *106*(D22), 28,567–28,575.
Müller, D., K. Franke, F. Wagner, D. Althausen, A. Ansmann, and J. Heintzenberg (2001b), Vertical profiling of optical and physical particle properties over the tropical Indian Ocean with six-wavelength lidar: 2. Case studies, *J. Geophys. Res.*, *106*(D22), 28,577–28,595.
Quinn, P. K., D. J. Coffman, T. S. Bates, T. L. Miller, J. E. Johnson, E. J. Welton, C. Neusüss, M. Miller, and P. J. Sheridan (2002), Aerosol optical properties during INDOEX 1999: Means, variability, and controlling factors, *J. Geophys. Res.*, *107*(D19), 8020, doi:10.1029/2000JD000037.
Rasch, P. J., W. D. Collins, and B. E. Eaton (2001), Understanding the Indian Ocean Experiment (INDOEX) aerosol distributions with an aerosol assimilation, *J. Geophys. Res.*, *106*(D7), 7337–7355.
Reddy, M. S., and O. Boucher (2004), Global carbonaceous aerosol transport and assessment of radiative effects in the LMDZ GCM, *J. Geophys. Res.*, *109*, D14202, doi:10.1029/2003JD004048.
Reddy, M. S., and C. Venkataraman (2002a), Inventory of aerosol and sulphur dioxide emissions from India: I. Fossil fuels combustion, *Atmos. Environ.*, *36*, 677–697.
Reddy, M. S., and C. Venkataraman (2002b), Inventory of aerosol and sulphur dioxide emissions from India: II. Biomass combustion, *Atmos. Environ.*, *36*, 699–712.
Reddy, M. S., O. Boucher, C. Venkataraman, S. Verma, J.-F. Leon, and M. Pham (2004), GCM estimates of aerosol transport and radiative forcing during INDOEX, *J. Geophys. Res.*, *109*, D16205, doi:10.1029/2004JD004557.
Satheesh, S. K., K. K. Moorthy, Y. J. Kaufman, and T. Takemura (2005), Aerosol optical depth, physical properties and radiative forcing over the Arabian Sea, *J. Meteorol. Atmos. Phys.*, *91*, 45–62, doi:10.1007/s00703-004-0097-4.
Satheesh, S. K., J. Srinivasan, and K. K. Moorthy (2006), Spatial and temporal heterogeneity in aerosol properties and radiative forcing over Bay of Bengal: Sources and role of aerosol transport, *J. Geophys. Res.*, *111*, D08202, doi:10.1029/2005JD006374.
Simon, M., S. Plummer, F. Fierens, J. J. Hoelzemann, and O. Arino (2004), Burnt area detection at global scale using ATSR-2: The GLOBSCAR products and their qualification, *J. Geophys. Res.*, *109*, D14S02, doi:10.1029/2003JD003622.
Streets, D. G., et al. (2003), An inventory of gaseous and primary aerosol emissions in Asia, *J. Geophys. Res.*, *108*(D21), 8809, doi:10.1029/2002JD003093.
Tansey, K., et al. (2004), Vegetation burning in the year 2000: Global burned area estimates from SPOT VEGETATION data, *J. Geophys. Res.*, *109*, D14S03, doi:10.1029/2003JD003598.
Tegen, I., and I. Fung (1995), Contribution to the atmospheric mineral aerosol load from land surface modification, *J. Geophys. Res.*, *100*(D9), 18,707–18,726.
Tiedtke, M. (1989), A comprehensive mass flux scheme for cumulus parameterization in large-scale models, *Mon. Weather Rev.*, *107*, 1779–1800.
van Leer, B. (1977), Towards the ultimate conservative difference scheme: IV. A new approach to numerical convection, *J. Comput. Phys.*, *23*, 276–299.
Venkataraman, C., G. Habib, A. Eiguren-Fernandez, A. H. Miguel, and S. K. Friedlander (2005), Residential biofuels in South Asia: Carbonaceous aerosol emissions and climate impacts, *Science*, *307*, 1454–1456.
Venkataraman, C., G. Habib, D. Kadamba, M. Shrivastava, J.-F. Leon, B. Crouzille, O. Boucher, and D. G. Streets (2006), Emissions from open biomass burning in India: Integrating the inventory approach with high-resolution moderate resolution imaging spectroradiometer (MODIS) active-fire and land cover data, *Global Biogeochem. Cycles*, *20*, GB2013, doi:10.1029/2005GB002547.
Verma, S., O. Boucher, C. Venkataraman, M. S. Reddy, D. Müller, P. Chazette, and B. Crouzille (2006), Aerosol lofting from sea breeze during the Indian Ocean Experiment, *J. Geophys. Res.*, *111*, D07208, doi:10.1029/2005JD005953.
Verma, S., C. Venkataraman, O. Boucher, and S. Ramachandran (2007), Source evaluation of aerosols measured during the Indian Ocean Experiment using combined chemical transport and back trajectory modeling, *J. Geophys. Res.*, *112*, D11210, doi:10.1029/2006JD007698.
Verver, G., D. R. Sikka, J. M. Lobert, G. Stossmeister, and M. Zachariasse (2001), Overview of the meteorological conditions and atmospheric transport processes during INDOEX 1999, *J. Geophys. Res.*, *106*(D22), 28,399–28,414.
Vinoj, V., A. Anjan, M. Sudhakar, S. K. Satheesh, J. Srinivasan, and K. K. Moorthy (2007), Latitudinal variation of aerosol optical depths from northern Arabian Sea to Antarctica, *Geophys. Res. Lett.*, *34*, L10807, doi:10.1029/2007GL029419.

O. Boucher, Met Office Hadley Centre, FitzRoy Road, Exeter EX1 3PB, UK. (olivier.boucher@metoffice.gov.uk)
C. Venkataraman, Department of Chemical Engineering, Indian Institute of Technology, Bombay, Mumbai 400 076, India. (chandra@iitb.ac.in)
S. Verma, Department of Civil Engineering, Indian Institute of Technology Kharagpur, Kharagpur 721 302, India. (shubha@iitkgp.ac.in)